**Title**

# Intra-articular AAV-PHP.S mediated chemogenetic targeting of knee-innervating dorsal root ganglion neurons alleviates inflammatory pain in mice.

**Authors**

Sampurna Chakrabarti[1], Luke A. Pattison [1], Balint Doleschall[2], Rebecca H. Rickman[1], Helen Blake[1], Gerard Callejo[1], Paul A. Heppenstall[2]†, Ewan St. John Smith[1*].

**Affiliations**.

1. Department of Pharmacology, University of Cambridge, UK.
2. European Molecular Biology Laboratory, Rome, Monterotondo, Italy.

† Present address: Scuola Internazionale Superiore di Studi Avanzati, via Bonomea, 265 - 34136 Trieste, Italy

* Corresponding author: Ewan St. John Smith, Department of Pharmacology, University of Cambridge, Tennis Court Road, Cambridge CB2 1PD. Email: es336@cam.ac.uk

**Abstract**

Objective:

Joint pain is the major clinical symptom of arthritis that affects millions of people. Controlling the excitability of knee-innervating dorsal root ganglion (DRG) neurons (knee neurons) could potentially provide pain relief. Therefore, our objective was to evaluate whether the newly engineered adeno-associated virus (AAV) serotype, AAV-PHP.S, can deliver functional artificial receptors to control knee neuron excitability following intra-articular knee injection.

Methods:

AAV-PHP.S virus packaged with dTomato fluorescent protein and either excitatory ($G_q$) or inhibitory ($G_i$) designer receptors activated by designer drugs (DREADDs) was injected into the knee joint of adult mice. Labelling of DRG neurons by AAV-PHP.S from the knee was evaluated using immunohistochemistry. Functionality of $G_q$- and $G_i$-DREADDs was evaluated using whole-cell patch clamp electrophysiology on acutely cultured DRG neurons. Pain behavior in mice was assessed using a digging assay, dynamic weight bearing and rotarod, before and after intra-peritoneal administration of the DREADD activator, Compound 21.

Results:

We show that AAV-PHP.S can deliver functional genes into the DRG neurons when injected into the knee joint in a similar manner to the well-established retrograde tracer, fast blue. Short-term activation of AAV-PHP.S delivered Gq-DREADD increases excitability of knee neurons in vitro, without inducing overt pain in mice when activated in vivo. By contrast, in vivo $G_i$-DREADD activation alleviated complete Freund's adjuvant mediated

knee inflammation-induced deficits in digging behavior, with a concomitant decrease in knee neuron excitability observed in vitro.

Conclusions

We describe an AAV-mediated chemogenetic approach to specifically control joint pain, which may be utilized in translational arthritic pain research.

## Introduction

Peripheral sensitization, manifested by an increase in the excitability of dorsal root ganglion (DRG) neurons, underlies many chronic pain pathologies, such as inflammatory arthritis (1). DRG neurons display great heterogeneity, based upon both gene expression (2,3) and functional attributes (4), and this heterogeneity is further compounded by target innervation (5,6). The variation in DRG neurons offers a unique opportunity to selectively tune the excitability of a distinct subset of DRG neurons in order to provide pain relief with reduced side-effects. For example, we have recently shown that the excitability of knee-innervating DRG neurons (identified by retrograde tracing) is increased in a mouse model of inflammatory joint pain (7) and after incubation with human osteoarthritis (OA) synovial fluid samples (8) . These results suggest that modulation of the knee-innervating DRG neuron subset (knee neurons) could help control arthritic pain.

One way of modulating neuronal excitability is to induce expression of inhibitory or excitatory designer receptors exclusively activated by exogenous chemical actuators which by themselves do not have any endogenous effects. Modified muscarinic receptor based designer receptors activated by designer drugs (DREADDs) is a technology based on this principle that can increase or decrease neuronal (mostly in the central nervous system, CNS) firing, which consequently affects a variety of behaviors (reviewed in (9,10)), such as enhanced feeding (11) or decreased wakefulness (12). In the peripheral nervous system (PNS), activation of the inhibitory DREADD $hM_4D(G_i)$ in voltage-gated sodium channel 1.8 ($Na_V1.8$) expressing DRG neurons decreased knee hyperalgesia and mechanical allodynia, along with a decrease in DRG neuron firing, in mice with early experimental OA pain induced by surgical destabilization of the medial meniscus (13). This attenuation of hyperalgesia was at a similar level when compared

to administration of 10 mg/kg morphine, thus suggesting that peripherally acting analgesics can be comparably potent to well-established opioids. Similarly, activating $G_i$-DREADD in transient receptor potential vanilloid 1 (TRPV1) expressing DRG neurons (14) increased the heat pain threshold and reduced neuronal excitability in mice. Both of these studies used transgenic mice and therefore are less translatable across species due to the technical difficulties associated with targeting sensory neuron sub-populations in species without such transgenic tractability. In wild-type mice, $G_i$-DREADD delivered intraneurally to the sciatic nerve via adeno-associated virus 6 (AAV6) was able to increase both mechanical and thermal thresholds (15). Importantly however, none of these studies were specific to DRG neuron subsets innervating specific organs.

AAVs are useful tools for gene transfer that have been used for gene therapy in a variety of human diseases (16), with multiple AAV-based clinical trials currently underway for arthritis (Clinical trial # NCT02727764, NCT02790723 (17)). AAVs can be utilized in conjunction with DREADD technology to selectively modulate neuronal activity of specific neuronal circuitry. Indeed, this has been achieved in the CNS (18). However, delivering genes by AAV injection into a peripheral organ to DRG neurons is challenging because of the low transduction capability of AAVs and the large anatomical distances involved in the PNS (19). A variety of AAV serotypes have shown little efficacy in transducing DRG neurons when injected sub-cutaneously, intra-muscularly or intra-plantarly in adult mice (20,21). To date direct injection into DRG (22) or intrathecal injection (23,24) are the best ways for transducing DRG neurons, however, these routes of administration are invasive, technically complicated to perform and do not enable transduction of neurons innervating a defined target. In the present study, we provide evidence that the PNS specific AAV serotype, AAV-PHP.S (19), can infect DRG

neurons with functional cargo following injection into the knee joint. Furthermore, using the inhibitory DREADD, $hM_4D(G_i)$, as a cargo, we show that its activation normalizes the inflammatory pain induced deficit in digging behavior in mice, which is an ethologically relevant spontaneous pain measure indicating well-being (25). This study thus extends the use of AAV and DREADD technologies to study DRG neurons infected from a peripheral organ, which can have future clinically-relevant applications in controlling pain pathologies.

## Materials and Methods

### Animals

10-15 week old C57BL/6J (Envigo) mice (n = 30) of both sexes were used in this study. Mice were housed in groups of up to 5 in a temperature controlled (21 °C) room on a 12-hour/light dark cycle with food, water and appropriate enrichment available *ad libitum.* Mice used in this study were regulated under the Animals (Scientific Procedure) Act 1986, Amendment Regulations 2012. All protocols were approved by a UK Home Office project license (P7EBFC1B1) and reviewed by the University of Cambridge Animal Welfare and Ethical Review Body.

### Viruses

AAV-PHP.S-CAG-tdTomato (Addgene #59462-PHP.S) was purchased from Addgene. AAV plasmids for DREADD viruses were purchased from Addgene (Table S1) and packaged at the European Molecular Biology Laboratory, Rome as has been described previously (26). Briefly, ten 150 mm dishes of HEK293T (ATCC) cells were triple transfected with plasmids (Table S1) of AAV-PHP.S, helper (Agilent) and cargo in a 1:4:1 ratio with PEI reagent (1:3 plasmid to PEI ratio, Sigma). Three days after transfection, cells and media were collected and this mixture was centrifuged at 3700xg at 4°C to remove debris and then concentrated by ultrafiltration using Vivaflow 200 (Sartorius). The purified AAV particles were collected after running the viral concentrate through an iodixanol column (Opti-Prep density gradient medium, Alere Technologies) by ultracentrifugation (Beckmann, L8-70M) at 44400xg for 2 hr at 18 °C

followed by filtration using a 100 kDa filter to further concentrate the sample and for buffer exchange. Viral titres (vg/ml) were measured by probing for WPRE regions (forward: GGCTGTTGGGCACTGACAAT, reverse: CCGAAGGGACGTAGCAGAAG) using SyBR green qPCR of linearized virus particles as described previously (26) using a StepOnePlus Real Time PCR system, following the manufacturer's guidelines on settings (Applied Biosystems).

Knee injections

All knee injections were conducted under anesthesia (100 mg/kg ketamine and 10 mg/kg xylazine, intra-peritoneally) through the patellar tendon. For experiments with retrograde tracing, 1.5 µl of fast blue (FB) or titer-matched AAV-PHP.S viruses were injected intra-articularly into knee joints (~$4x10^{11}$ vg of AAV-PHP.S-CAG-dTomato and ~$5x10^{11}$ vg of AAV-PHP.S packaged with $G_i$ and $G_q$-DREADD into each knee). The titer values were chosen based on a pilot experiment conducted with AAV-PHP.S-CAG-YFP, injection of 2 ul (~$3x10^{11}$ vg) and 10 ul (~$10^{\wedge 12}$ vg) labelled a similar number of neurons as assessed by acute culture. For experiments involving inflammation, 7.5 µl CFA (10 mg/ml, Chondrex) was injected into the left knee and Vernier's calipers were used to measure knee width (as before (7)) pre- and 24-hour post-CFA injection.

Behavioral testing

All behavioral experiments were carried out between 10:00 and 13:00 in the presence of one male and one female experimenter. Mice were assigned randomly to control and experimental groups and at least two cohorts of mice (8-12 mice in each group) were assessed in each group

on separate days. Mice were trained on digging and rotarod one day before the test days. The following groups were tested in this study:

1. **Compound 21 (C21) controls:** Behavioral tests (described below) were performed on mice with no knee injections 20 min before and after C21 (2 mg/kg diluted in sterile saline from a stock of 100 mM in ethanol, i.p., Tocris) injection.
2. **Activation of $G_q$-DREADD:** 3-4 weeks after intra-articular administration of virus, mice were behaviorally tested 20 min before and after vehicle (1:100 ethanol in sterile saline) or C21 injections.
3. **Activation of $G_i$-DREADD:** 3-4 weeks after intra-articular administration of virus, baseline behavioral tests were conducted on mice (pre-CFA). CFA was injected into the knee joints the next day to induce inflammation. 24-hours after that, animals were re-tested 20 min before (post-CFA) and after (post-C21) vehicle or C21 injections.

Digging

Digging behavior was measured as an assessment of spontaneous pain as described before (7) for three min in a standard cage with a wire lid, filled with Aspen midi 8/20 wood chip bedding (LBS Biotechnology). For training, mice were habituated in the test room in their home cages for 30 min then they were allowed to dig twice for 3 min with 30 min break in between. On each subsequent test day, mice were habituated and tested once on the 3 min paradigm. Test sessions were video recorded from which the digging duration was later independently coded by the experimenters, blinded to the conditions. Number of dig sites (burrows) was coded on test days by the experimenters.

Rotarod

Locomotor function and coordination of mice were tested using a rotarod apparatus (Ugo Basile 7650). Mice were tested on a constant speed rotarod at 7 rpm for 1 min, then in an accelerating program (7-40 rpm in 5 min) for 6 min. The same protocol was used to train mice one day before testing. Mice were removed from the rotarod after two passive rotations or when they fell from the rotarod. Mice were video recorded on test days and one experimenter blinded to the conditions coded these videos for latency(s) to passive rotation or fall.

Dynamic weight bearing

Deficit in weight bearing capacity is a characteristic measure of spontaneous inflammatory pain behavior and we measured this behavior using a dynamic weight bearing (DWB) device (Bioseb) in freely moving mice for 3 min. Animals were not trained in this device and coding was done by one experimenter, blinded to the conditions. In at least 1 min 30 sec of the 3 min recording, fore- and hind paw prints were identified using the two highest confidence levels (based on correlation between manual software algorithm tracking) of the in-built software, at least 30 s of which was manually verified.

DRG neuron culture

Lumbar DRG (L2-L5) were collected from a subset of mice in the vehicle group 3-4 weeks after virus injections in ice cold dissociation media (as before (7)). DRG were then enzymatically digested followed by mechanical trituration (7). Dissociated DRG neurons, thus isolated, were then plated onto poly-D-lysine and laminin coated glass bottomed dishes (MatTek, P35GC-1.5-14-C) in DRG culture medium contained L-15 Medium (1X) + GlutaMAX-l, 10% (v/v) fetal bovine serum, 24 mM $NaHCO_3$, 38 mM glucose, 2%

penicillin/streptomycin and maintained overnight (8-10-hours) in a humidified, 37 °C, 5% $CO_2$ incubator before recording.

Electrophysiology

For control experiments, DRG neurons were bathed in extracellular solution containing (ECS, in mM): NaCl (140), KCl (4), $MgCl_2$ (1), $CaCl_2$ (2), glucose (4) and HEPES (10) adjusted to pH 7.4 with NaOH while recording. To investigate effects of C21 activation, neurons were incubated 10 min prior to the start of recording and throughout the recordings in 10 nM C21 (diluted in ECS from 100 mM stock). Only virus transduced mice identified by their fluorescence upon excitation with a 572 nm LED (Cairn Research) were recorded using patch pipettes of 5–10 MΩ (P-97 Flaming/Brown puller, Sutter Instruments) containing intracellular solution (in mM): KCl (110), NaCl (10), $MgCl_2$ (1), EGTA (1), HEPES (10), $Na_2ATP$ (2), $Na_2GTP$ (0.5) adjusted to pH 7.3 with KOH.

Action potentials (AP) were recorded in current clamp mode without current injection (to investigate spontaneous AP firing) or after step-wise injection of 80 ms current pulses from 0 – 1050 pA in 50 pA steps using a HEKA EPC-10 amplifier (Lambrecht) and the corresponding Patchmaster software. AP properties were analysed using Fitmaster software (HEKA) or IgorPro software (Wavemetrics) as described before (7). Neurons were excluded from analysis if they did not fire an AP in response to current injections.

Immunohistochemistry

Mice with unilateral, co-injections of AAV-PHP.S-tdTomato (2 ul) and FB (1.5 ul) were transcardially perfused with 4% (w/v) paraformaldehyde (PFA; in PBS, pH 7.4) under terminal

anesthesia (sodium pentobarbital, 200 mg/kg, i.p.). L2-L5 DRG were then collected from the injected side, while L3-L4 were collected from the non-injected side and post-fixed in Zamboni's fixative for 1-hour, followed by overnight incubation in 30% (w/v) sucrose (in PBS) at 4 °C for cryo-protection. DRG were then embedded, snap-frozen, sectioned and stained as described previously (7) using anti-TRPV1 antibody (1:500, Alomone, AGP-118, anti-guinea pig polyclonal) with Alexa-488 conjugated secondary antibody (1:500, Jackson Laboratory, 706-545-148, anti-guinea pig). Positive neurons were scored as has been reported previously (7) using a R toolkit (https://github.com/amapruns/Immunohistochemistry_Analysis) followed by manual validation. Briefly, mean grey value (intensity) of all neurons on 1-3 sections from each DRG level of interest from each mouse was measured using ImageJ. A neuron was scored positive for a stain if it had an intensity value greater than average normalized minimum grey value across all sections + 2 times the standard deviation.

Statistics

Comparisons between two groups were made using appropriate (paired for repeated measures and unpaired otherwise) Student's t-test while three group comparisons were made using one-way analysis of variance (ANOVA) followed by Holm-Sidak multiple comparison tests. Chi-sq tests were utilized to compare proportions of categorical variables. Data are presented as mean ± standard error of mean.

## Results

### 1. Knee injected AAV-PHP.S robustly transduces DRG neurons

AAV-PHP.S was engineered to have a higher specificity towards peripheral neurons (19) and thus we hypothesized that this AAV serotype would be able to transduce DRG neurons when injected intra-articularly into the knee joint. Consistent with our hypothesis, when AAV-PHP.S-CAG-dTomato and the commonly used retrograde tracer fast blue (FB) were co-injected unilaterally into one knee of mice (n = 3, female), we observed both FB and virus labelling (Fig 1A). In agreement with previous reports using FB and other retrograde tracers (7,27,28), we observed a similar proportion of labelling in the lumbar DRG with FB and AAV-PHP.S-CAG-dTomato (Fig 1B). Across L2-L5 DRG, there was ~ 40 % co-labelling of neurons with FB and AAV-PHP.S-CAG-dTomato suggesting that neither retrograde tracer is able to label the entire knee neuron population (Fig 1C, Fig S1). However, area analysis of the labelled neurons suggests that similar sized neurons are targeted by both strategies (Fig S1). Furthermore, we observed minimum labelling in the contralateral side (Fig S1). Previous reports suggest that ~40 % of knee neurons are TRPV1 expressing putative nociceptors (7,28). Similarly, with immunohistochemistry analysis of DRG neurons, we find that ~30 % of viral labelled and FB labelled neurons (mostly small diameter neurons) express TRPV1 (Fig 1D, Fig S1) suggesting that viral transduction did not substantially alter expression of the nociceptive protein, TRPV1. Taken together, we find that intra-articular injection of AAV-PHP.S-CAG-dTomato in the knee joint transduces mouse DRG neurons in a similar manner to a routinely used retrograde tracer.

### 2. Excitatory $G_q$-DREADD delivered intra-articularly by AAV-PHP.S-hSyn-h$M_3$D($G_q$)-mCherry does not change spontaneous pain behavior, but provokes a deficit in motor coordination.

Next we tested whether AAV-PHP.S can deliver functional $hM_3D(G_q)$ cargo into knee neurons via intra-articular injection, using whole-cell patch clamp on acutely dissociated neurons isolated from mice with no previous exposure to the DREADD activator Compound (C21). C21 was chosen as the DREADD activator since it has good bioavailability (plasma concentration measured to be at 57% 1 hour post injection), is not converted into clozapine or clozapine-N-oxide (29) and had no off-target effect in the behavioral tests conducted in this study in naïve mice not injected with DREADDs (Fig S2). $G_q$-DREADDs couple to $G_q$PCR pathways and thus their activation causes neuronal excitation (9). Therefore, we hypothesized that when incubated with 10 nM C21, virally transduced neurons would be hyperexcitable compared to virally transduced neurons bathed in normal extracellular solution (ECS). In agreement with this hypothesis, we observed an increased number of mostly small and medium diameter (Fig S3) mostly nociceptive (characterized by having an AP half peak duration > 1 ms and with a "hump" during repolarization, Fig S3, (30)) neurons (Ctrl, 5.3% vs. C21, 27.8% $p = 0.03$, chi-sq test) firing action potentials (AP) without injection of current in the C21 group (Fig 2A,B, S3). Moreover, upon injection of increasing stepwise current injections, the action potential (AP) threshold was decreased ($p = 0.02$, unpaired t-test) in the C21 group (Fig 2C); no change was observed in other electrical properties measured in these neurons (Table 1). Our data also suggest that virally transduced neurons are viable because the reported AP threshold is very similar to what we have observed previously in FB+ knee-innervating neurons (31).

Based on previous studies (7,8), we hypothesized that the measured increased excitability of knee-innervating neurons in vitro via the $G_q$-DREADD system would cause pain-like behavior in mice in vivo, which was tested by measuring digging behavior (a measure of spontaneous pain as described previously (7,30)), dynamic weight bearing and rotarod behavior (a measure

of motor co-ordination) (31) (Timeline in Fig 2D). Three weeks after virus injection into both knee joints, mice (n = 8, 4 males, 4 females in each group) injected with vehicle or C21 did not show changes in digging behavior (Digging duration: Pre vs. Post veh, 31.6 ± 3.7 ms vs. 21.3 ± 4.4 ms, Pre vs. Post C21, 25.2 ± 4.9 ms vs. 32.7 ± 4.7 ms; Number of burrows: Pre vs. Post veh, 4.6 ± 0.5 vs. 3.5 ± 0.4, Pre vs. Post C21, 3.9 ± 0.7 vs. 3.6 ± 0.5, Fig 2E,F) or weight bearing (Front/Rear paw weight ratio: Pre vs. Post veh, 0.5 ± 0.02 vs. 0.5 ± 0.04, Pre vs. Post C21, 0.4± 0.06 vs. 0.4 ± 0.03, Fig 2G,H). By contrast, after injection of C21, mice showed a marked decline in their ability to remain on the rotarod (Pre vs. Post veh, 273.5 ± 27.2 s vs. 243.9 ± 32.7 s, Pre vs. Post C21, 336.1 ± 12.9 s vs. 249.0 ± 18.9 s, p = 0.002, paired t-test) suggesting a deficit in their motor co-ordination (Fig 2I,J). DRG for all virus injected mice were visualized under a fluorescence microscope to check for viral transduction and a subset of these DRG were further analyzed to reveal similar transduction profiles between AAV-PHP.S-hSyn-$G_q$DREADD-mCherry and AAV-PHP.S-CAG-dTomato (Fig S3), i.e. different promoters do not significantly affect transduction.

Taken together, our data show that AAV-PHP.S delivers functional $G_q$-DREADD into knee neurons and that when virally transduced knee neurons are activated they do not produce overt pain-like behavior in vivo, but do cause a deficit in motor coordination.

### 3. Inhibitory $G_i$-DREADD delivered intra-articularly by AAV-PHP.S-hSyn-hM$_4$D($G_i$)-mCherry reverses digging behavior deficits associated with inflammatory pain.

Intra-articular injection of complete Freund's adjuvant (CFA) induces robust knee inflammation in mice (Ctrl knee: pre CFA day, 3.1 ± 0.03 mm, post CFA day, 3.1 ± 0.03 mm;

CFA knee: pre CFA day, 3.1 ± 0.02 mm, post CFA day, 4.0 ± 0.05 mm, n = 24, $p < 0.0001$, paired t-test, Fig 3A,B) and has been previously shown to increase the excitability of knee neurons innervating the inflamed knee compared to those innervating the contralateral side (7). The post-CFA knee measurements were conducted at the end of behavioral measurements, thus suggesting that regardless of $G_i$-DREADD activation knee inflammation persisted at 24-hour post-CFA injection.

We hypothesized that incubating $G_i$-DREADD expressing knee neurons from the CFA side with C21 would reverse this increased neuronal excitability. Using whole-cell patch clamp electrophysiology of small and medium diameter (Fig S4) knee neurons, although there was no change in the resting membrane potential across any condition (Fig 3C, Table 2), the percentage of CFA knee neurons firing spontaneous AP decreased after $G_i$-DREADD activation (CFA, 15% vs. CFA+ C21, 0%, $p = 0.02$, chi-sq test, Fig 3C,S3). Moreover, in the absence of $G_i$-DREADD activation, CFA knee neurons had a decreased AP threshold compared to neurons from the control side, but the AP threshold of CFA knee neurons that were incubated in C21 was similar to that of neurons from the control side ($p = 0.005$, ANOVA, Fig 3D). These results suggest that $G_i$-DREADD activation reverses CFA-induced increase in nociceptor (based upon the criteria mentioned above, Fig S4) excitability in vitro. Other electrical properties between groups were unchanged (Table 2).

The ability of $G_i$-DREADD to modulate pain behavior in DRG neurons is unclear with one study showing an increase in latency to both thermal and mechanical stimuli (15), but another showing only an increase in the paw withdrawal latency to thermal stimuli (14). Nevertheless, based on the in vitro results in these studies, we hypothesized that activation of $G_i$-DREADDs

in knee neurons post CFA would reverse spontaneous pain behavior in mice (timeline in Fig 3E). In the control cohort of mice (n = 9, 5 males, 4 females) that received vehicle 24-hours after CFA injection, the CFA-induced decrease in digging behavior persisted compared to pre CFA (Digging duration: Pre CFA, 29.6 ± 2.7 ms, post CFA 16.6 ± 4.0 ms, post veh, 9.8 ± 2.8 ms, $p = 0.0005$, repeated measures ANOVA; Number of burrows: Pre CFA, 4.8 ± 0.3, post CFA 2.9 ± 0.3 ms, post veh, 2.3 ± 0.5 ms, n = 9, $p < 0.0001$, repeated measures ANOVA, Fig 3F). However, when C21 was administered to a separate cohort of mice (n = 11, 7 males, 4 females) 24-hours after CFA injection, there was a marked recovery in digging behavior (Digging duration: Pre CFA, 29.7 ± 4.5 ms, post CFA 7.8 ± 1.9 ms, post C21, 19.0 ± 3.9 ms, $p = 0.0002$, repeated measures ANOVA; Number of burrows: Pre CFA, 4.5 ± 0.3, post CFA 2.4 ± 0.3 ms, post C21, 3.6 ± 1.4 ms, $p = 0.0005$, repeated measures ANOVA, Fig 3G) suggesting that decreasing the excitability of knee neurons via $G_i$-DREADD reduces inflammation induced spontaneous pain that is associated with an increase in the feeling of well-being demonstrated by more digging. In contrast, acute chemogenetic inhibition of knee neurons was insufficient to reverse the CFA-induced deficit in dynamic weight bearing (Rear left weight bearing as % of body weight: Pre CFA, 26.2 ± 2.0, post CFA, 10.6 ± 1.7, post veh, 11.6 ± 1.5, $p < 0.0001$; Pre CFA, 26.1 ± 1.1, post CFA, 12.4 ± 1.4, post C21, 13.3 ± 2.2, $p < 0.0001$, repeated measures ANOVA, Fig 3H,I) which might be because gait changes relating to weight bearing is more reflective of changes in joint biomechanics that are difficult to reverse by analgesics (32). Furthermore, no change in rotarod behavior was observed following CFA-induced knee inflammation suggesting that this model does not cause an overt change in gross motor function and similarly $G_i$-DREADD activation also had no effect (Pre CFA, 303.8 ± 18.3 s, post CFA, 315.9 ± 11.9 s, post veh, 306.6 ± 16.8 s; Pre CFA, 282.7 ± 17.3 s, post CFA, 286.4 ± 25.3 s,

post C21, 317.4 ± 10.3 s, Fig 3J,K). DRG for all virus injected mice were visualized under a fluorescence microscope to check for viral transduction (Fig S4).

Taken together, our results suggest that specific inhibition of knee neuron excitability can reverse inflammation-induced deficit in digging behavior.

## Discussion

The findings in this study show that the AAV-PHP.S serotype can retrogradely deliver cargo to DRG neurons in a peripheral tissue-specific manner when injected into the knee joints without the need for invasive procedures or the requirement to generate transgenic mice. The transduction efficacy of the virus is similar to the widely used retrograde tracer, FB. In-line with other co-labelling studies (33), the ~40% co-localization of AAV-PHP.S and FB fluorescence suggests that not all knee neurons are labeled by either tracer and the less than 100% co-labeling is possibly due to their differing modes of retrograde transfer (34,35). Furthermore, we report that ~30% of labelled neurons are TRPV1+, which fits with the previously reported identity of knee-innervating neurons as a subset being ~39% TRPV1+, ~53% CGRP+ and largely IB4 non-binding (28,39).

Using this system, we show that it is possible to increase or decrease knee neuron excitability in vitro when $G_q$ or $G_i$-DREADD cargoes were delivered by AAV-PHP.S respectively and hence provide joint specific pain control. This result can also be extended to study the role of anatomically specific neuronal excitability when exposed to a variety of stimuli or pharmacological interventions. In vivo, we restricted our chemogenetic activation to a short duration to reflect acute pain and within this timeframe saw no spontaneous pain-like behavior with activation of $G_q$-DREADD in knee neurons. We surmise that $G_q$-mediated sub-threshold activation (36) of the relatively low percentage of DRG neurons did not provide sufficient nociceptive input to drive change in ethologically relevant pain behavior; whereas the observed decrease in coordination suggests that we have behaviorally engaged the virally transduced neurons. Furthermore, we note that intra-articular injection described here would transduce DREADDs to both nociceptive and non-nociceptive population of knee neurons, therefore, a clear nocifensive behavior might not be apparent, i.e. a limitation of this study is that distinct subpopulations of knee neurons are not

targeted, but future studies could address this once such populations have been described for the knee as has already been conducted for the colon (5). Future studies using a repeated dosing strategy could also be employed in our system for modelling chronic pain, being cautious of the potential risk of receptor desensitization (9).

Perhaps more relevant to future clinical applications in arthritic pain is the ability of $G_i$-DREADDs to reverse pain behavior by decreasing neuronal excitability of knee neurons. Indeed, we show that $G_i$-DREADD activation restores a deficit in digging behavior induced by inflammatory knee pain, similar to previous reports demonstrating normalization of burrowing/digging by non-steroidal anti-inflammatory drugs (41,42) and a peripherally restricted TRPV1 antagonist (7) after joint pain induced depression of this behavior. This strategy can be further refined to selectively inhibit genetically specific subpopulation of knee neurons by combining Cre-inducible viruses with their corresponding Cre-expressing transgenic mouse lines, and hence provide insights into relative contributions of different knee neuron sub-populations in arthritic pain. Selectively exciting specific knee neuron sub-populations with $G_q$-DREADD might also produce pain-like behaviors that were not observed in this study. We also report that the CFA-induced deficit in weight bearing was not reversed following activation of $G_i$-DREADD in knee neurons, consistent with a previous report observing that reversal of deficits in gait changes are difficult to achieve with analgesics (32).

Although findings from this study imply that modulating excitability of anatomically specific peripheral neurons could control arthritic pain, a number of challenges remain to be addressed before their clinical translation. Since virus transduction and expression profile is different between non-human primates and rodents, the expression profile of AAV-PHP.S needs to be first validated in non-human primates (37). Additional work is also required to engineer more

PNS specific AAVs and to optimize DREADDs (38) and their corresponding ligands (39) for increasing transduction efficiency and regulating dosing.

Overall, the present study provides initial proof-of-concept that peripheral tissue innervating DRG neurons can be specifically modulated by AAVs, opening the door to future studies on gene therapy in controlling arthritic pain.

## References


1. Walsh DA, McWilliams DF. Mechanisms, impact and management of pain in rheumatoid arthritis. *Nature Reviews Rheumatology* 2014;10:581–592.

2. Zeisel A, Hochgerner H, Lönnerberg P, Johnsson A, Memic F, Zwan J van der, et al. Molecular Architecture of the Mouse Nervous System. *Cell* 2018;174:999-1014.e22.

3. North RY, Li Y, Ray P, Rhines LD, Tatsui CE, Rao G, et al. Electrophysiological and transcriptomic correlates of neuropathic pain in human dorsal root ganglion neurons. *Brain* 2019;142:1215–1226.

4. Petruska JC, Napaporn J, Johnson RD, Gu JG, Cooper BY. Subclassified Acutely Dissociated Cells of Rat DRG: Histochemistry and Patterns of Capsaicin-, Proton-, and ATP-Activated Currents. *Journal of Neurophysiology* 2000;84:2365–2379.

5. Hockley JRF, Taylor TS, Callejo G, Wilbrey AL, Gutteridge A, Bach K, et al. Single-cell RNAseq reveals seven classes of colonic sensory neuron. *Gut* 2019;68:633.

6. Immke DC, McCleskey EW. Lactate enhances the acid-sensing Na+ channel on ischemia-sensing neurons. *Nature Neuroscience* 2001;4:869–870.

7. Chakrabarti S, Pattison LA, Singhal K, Hockley JRF, Callejo G, Smith EStJ. Acute inflammation sensitizes knee-innervating sensory neurons and decreases mouse digging behavior in a TRPV1-dependent manner. *Neuropharmacology* 2018;143:49–62.

8. Chakrabarti S, Jadon DR, Bulmer DC, Smith EStJ. Human osteoarthritic synovial fluid increases excitability of mouse dorsal root ganglion sensory neurons: an in-vitro translational model to study arthritic pain. *Rheumatology* 2020;59:662–667.

9. Roth BL. DREADDs for Neuroscientists. *Neuron* 2016;89:683–694.

10. Wood JN, Alles SRA, Malfait A-M, Miller RJ. *Chemo- and Optogenetic Strategies for the Elucidation of Pain Pathways*. Oxford University Press; 2019. Available at: https://www.oxfordhandbooks.com/view/10.1093/oxfordhb/9780190860509.001.0001/oxfordhb-9780190860509-e-33.

11. Krashes MJ, Koda S, Ye C, Rogan SC, Adams AC, Cusher DS, et al. Rapid, reversible activation of AgRP neurons drives feeding behavior in mice. *J Clin Invest* 2011;121:1424–1428.

12. Sasaki K, Suzuki M, Mieda M, Tsujino N, Roth B, Sakurai T. Pharmacogenetic modulation of orexin neurons alters sleep/wakefulness states in mice. *PLoS One* 2011;6:e20360–e20360.

13. Miller RE, Ishihara S, Bhattacharyya B, Delaney A, Menichella DM, Miller RJ, et al. Chemogenetic Inhibition of Pain Neurons in a Mouse Model of Osteoarthritis. *Arthritis Rheumatol* 2017;69:1429–1439.

14. Saloman JL, Scheff NN, Snyder LM, Ross SE, Davis BM, Gold MS. Gi-DREADD Expression in Peripheral Nerves Produces Ligand-Dependent Analgesia, as well as Ligand-Independent Functional Changes in Sensory Neurons. *J Neurosci* 2016;36:10769–10781.

15. Iyer SM, Vesuna S, Ramakrishnan C, Huynh K, Young S, Berndt A, et al. Optogenetic and chemogenetic strategies for sustained inhibition of pain. *Sci Rep* 2016;6:30570–30570.

16. Wang D, Tai PWL, Gao G. Adeno-associated virus vector as a platform for gene therapy delivery. *Nature Reviews Drug Discovery* 2019;18:358–378.

17. U.S. National library of medicine. Clinical Trials. 2019. Available at: https://clinicaltrials.gov/. Accessed January 12, 2019.

18. Aschauer DF, Kreuz S, Rumpel S. Analysis of Transduction Efficiency, Tropism and Axonal Transport of AAV Serotypes 1, 2, 5, 6, 8 and 9 in the Mouse Brain. *PLOS ONE* 2013;8:e76310.

19. Chan KY, Jang MJ, Yoo BB, Greenbaum A, Ravi N, Wu W-L, et al. Engineered AAVs for efficient noninvasive gene delivery to the central and peripheral nervous systems. *Nature neuroscience* 2017;20:1172–1179.

20. Towne C, Pertin M, Beggah AT, Aebischer P, Decosterd I. Recombinant adeno-associated virus serotype 6 (rAAV2/6)-mediated gene transfer to nociceptive neurons through different routes of delivery. *Mol Pain* 2009;5:52–52.

21. Abdallah K, Nadeau F, Bergeron F, Blouin S, Blais V, Bradbury KM, et al. Adeno-associated virus 2/9 delivery of Cre recombinase in mouse primary afferents. *Sci Rep* 2018;8:7321–7321.

22. Mason MRJ, Ehlert EME, Eggers R, Pool CW, Hermening S, Huseinovic A, et al. Comparison of AAV serotypes for gene delivery to dorsal root ganglion neurons. *Mol Ther* 2010;18:715–724.

23. Storek B, Harder NM, Banck MS, Wang C, McCarty DM, Janssen WG, et al. Intrathecal long-term gene expression by self-complementary adeno-associated virus type 1 suitable for chronic pain studies in rats. *Mol Pain* 2006;2:4–4.

24. Weir GA, Middleton SJ, Clark AJ, Daniel T, Khovanov N, McMahon SB, et al. Using an engineered glutamate-gated chloride channel to silence sensory neurons and treat neuropathic pain at the source. *Brain* 2017;140:2570–2585.

25. Jirkof P. Burrowing and nest building behavior as indicators of well-being in mice. *Journal of Neuroscience Methods* 2014;234:139–146.

26. Challis RC, Ravindra Kumar S, Chan KY, Challis C, Beadle K, Jang MJ, et al. Systemic AAV vectors for widespread and targeted gene delivery in rodents. *Nature Protocols* 2019;14:379–414.

27. Ferreira-Gomes J, Adães S, Sarkander J, Castro-Lopes JM. Phenotypic alterations of neurons that innervate osteoarthritic joints in rats. *Arthritis & Rheumatism* 2010;62:3677–3685.

28. Cho WG, Valtschanoff JG. Vanilloid receptor TRPV1-positive sensory afferents in the mouse ankle and knee joints. *Brain Research* 2008;1219:59–65.

29. Jendryka M, Palchaudhuri M, Ursu D, Veen B van der, Liss B, Kätzel D, et al. Pharmacokinetic and pharmacodynamic actions of clozapine-N-oxide, clozapine, and compound 21 in DREADD-based chemogenetics in mice. *Sci Rep* 2019;9:4522–4522.

30. Djouhri L, Lawson SN. Changes in somatic action potential shape in guinea-pig nociceptive primary afferent neurones during inflammation in vivo. *The Journal of Physiology* 1999;520:565–576.

31. Chakrabarti S, Pattison LA, Bhebhe CN, Callejo G, Bulmer DC, Smith EStJ. Sensitization of knee-innervating sensory neurons by tumor necrosis factor-α activated fibroblast-like synoviocytes: an in vitro, co-culture model of inflammatory pain. *bioRxiv* 2019:791251.

32. Chakrabarti S, Jadon DR, Bulmer DC, Smith EStJ. Human osteoarthritic synovial fluid increases excitability of mouse dorsal root ganglion sensory neurons: an in-vitro translational model to study arthritic pain. *Rheumatology* 2019. Available at: https://doi.org/10.1093/rheumatology/kez331. Accessed August 14, 2019.

33. Deacon RMJ. Digging and marble burying in mice: simple methods for in vivo identification of biological impacts. *Nature Protocols* 2006;1:122.

34. Tappe-Theodor A, King T, Morgan MM. Pros and Cons of Clinically Relevant Methods to Assess Pain in Rodents. *Neuroscience & Biobehavioral Reviews* 2019;100:335–343.

35. Shepherd AJ, Mohapatra DP. Pharmacological validation of voluntary gait and mechanical sensitivity assays associated with inflammatory and neuropathic pain in mice. *Neuropharmacology* 2018;130:18–29.

36. Puigdellívol-Sánchez A, Prats-Galino A, Ruano-Gil D, Molander C. Efficacy of the fluorescent dyes Fast Blue, Fluoro-Gold, and Diamidino Yellow for retrograde tracing to dorsal root ganglia after subcutaneous injection. *Journal of Neuroscience Methods* 1998;86:7–16.

37. Eisenman LM. Uptake of the retrograde fluorescent tracer Fast blue from the cerebrospinal fluid of the rat. *Neuroscience Letters* 1985;60:241–246.

38. Tervo DGR, Hwang B-Y, Viswanathan S, Gaj T, Lavzin M, Ritola KD, et al. A Designer AAV Variant Permits Efficient Retrograde Access to Projection Neurons. *Neuron* 2016;92:372–382.

39. Ivanavicius S, Blake D, Chessell I, Mapp P. Isolectin B4 binding neurons are not present in the rat knee joint. *Neuroscience* 2004;128:555–560.

40. Jaiswal PB, English AW. Chemogenetic enhancement of functional recovery after a sciatic nerve injury. *Eur J Neurosci* 2017;45:1252–1257.

41. Gould SA, Doods H, Lamla T, Pekcec A. Pharmacological characterization of intraplantar Complete Freund's Adjuvant-induced burrowing deficits. *Behavioural Brain Research* 2016;301:142–151.

42. Rutten K, Schiene K, Robens A, Leipelt A, Pasqualon T, Read SJ, et al. Burrowing as a non-reflex behavioural readout for analgesic action in a rat model of sub-chronic knee joint inflammation. *European Journal of Pain* 2014;18:204–212.

43. Galvan A, Raper J, Hu X, Paré J-F, Bonaventura J, Richie CT, et al. Ultrastructural localization of DREADDs in monkeys. *European Journal of Neuroscience* 2019;50:2801–2813.

44. Magnus CJ, Lee PH, Atasoy D, Su HH, Looger LL, Sternson SM. Chemical and genetic engineering of selective ion channel-ligand interactions. *Science* 2011;333:1292–1296.

45. Thompson KJ, Khajehali E, Bradley SJ, Navarrete JS, Huang XP, Slocum S, et al. DREADD Agonist 21 Is an Effective Agonist for Muscarinic-Based DREADDs in Vitro and in Vivo. *ACS Pharmacol Transl Sci* 2018;1:61–72.

## Acknowledgements

**General**: Authors would like to thank: Morris Poeuw and Fernanda Castro de Reis for technical help with viral production. Julie Gautrey and Anne Desevre for technical help with mouse behavior. Dewi Safitri for graphic design.

**Funding:** This study was supported by Versus Arthritis Project grants (RG 20930 and RG 21973) to E. St. J. S. and G.C. S.C. was supported by Gates Cambridge Trust scholarship, Cambridge Philosophical Society research fund, Department of Pharmacology (University of Cambridge) travel award and Corpus Christi College (University of Cambridge) travel award. L.A.P. was supported by the University of Cambridge BBSRC Doctoral Training Programme (BB/M011194/1). P.A.H and B.D. were supported by EMBL.

**Author contributions:** S.C. designed experiments, collected and analyzed data and wrote the manuscript. L.A.P. collected and analyzed behavioral data and revised the manuscript. B.D. helped with virus production. R.H.R. and H.B. helped with immunohistochemistry analysis. G.C. helped with behavioral experiments and revised the manuscript. P.A.H. and E. St. J. S. designed experiments and revised the manuscript. All authors approved the final version of the manuscript.

**Competing interests:** The authors declare no conflict of interest.

**Data and materials availability:** Data presented in this article will be available in the Cambridge University Apollo repository (https://doi.org/10.17863/CAM.46171).

## Figure Legends

**Fig. 1. Retrograde tracing of knee-innervating DRG neurons using FB and AAV-PHP.S-CAG-dTomato.** A) Representative images of a whole L3 DRG section showing knee neurons traced using FB (blue), AAV-PHP.S-CAG-dTomato (pink) and stained using an anti-TRPV1 antibody (yellow). White triangle is pointing at a neuron that had FB, AAV-PHP.S and TRPV1 colocalization, while the white arrow is pointing at a neuron that shows only FB and AAV-PHP.S co-localization. B) Bar graphs showing percent of labelled neurons in L2-L5 DRG with FB and AAV-PHP.S. Percent of neurons showing co-localization of FB and AAV-PHP.S (C), and TRPV1 and AAV-PHP.S (D), expressed as a percent of AAV-PHP.S$^{+}$ neurons. The error bars represent the SEM in the data obtained from three female mice.

**Fig. 2. $G_q$-DREADD activation of knee neurons in-vitro and in-vivo.** A) Representative image of an AAV-PHP.S-hSyn-hM$_3$D($G_q$)-mCherry transduced neuron (Scale bar = 25 μm, triangular shadow = recording electrode). B) bars showing resting membrane potential in Ctrl (black, n = 19) and C21 (blue, n = 18) conditions, pie-chart showing percent of neurons in each condition that fired spontaneous AP. C) Bars showing AP firing threshold in Ctrl (black, n = 19) and C21 (blue, n = 18) conditions, pie-chart showing percent of neurons in each condition that fired multiple AP upon current injection. *$p < 0.05$, unpaired t-test. Data obtained from 3 females and 2 male mice. D) Timeline showing when behaviors were conducted. Digging duration and burrows (along with schematic diagram), ratio of front and rear paw weight (along with schematic diagram) and rotarod behavior (along with schematic diagram) before and after vehicle (E, G, I) or C21 injection (F, H, J). ** $p < 0.01$, paired t-test. Data obtained from 4 female and 4 male mice. Error bars = SEM.

**Fig. 3. $G_i$-DREADD activation of knee neurons in vitro and in vivo.** A) Bars representing knee width before and after CFA injection in the non-injected (contra, black) and injected knee (ipsi, red), **** $p < 0.0001$, n = 20, paired t-test. B) Bars showing resting membrane potential in Ctrl (black, n = 22), CFA (red, n = 20) and CFA+C21 (blue, n = 22) conditions, pie-chart showing percent of neurons in CFA and CFA+C21 condition that fired spontaneous AP. C) Bars showing AP firing threshold in Ctrl (black, n = 22), CFA (red, n = 20) and CFA+C21 (blue, n = 22) conditions, pie-chart showing percent of neurons in CFA and CFA+C21 condition that fired multiple AP upon current injection. *$p < 0.05$, ***$p < 0.001$ ANOVA and Holm-Sidak multiple comparison test. Data obtained from 2 female and 2 male mice. D) Timeline showing when behaviors were conducted. Digging duration and number of burrows, rear left paw weight expressed as percent of body weight and rotarod behavior pre and post-CFA and after vehicle (E, G, I, 4 female and 5 male mice) or C21 injection (F, H, J, 4 female and 7 male mice). *$p < 0.05$, ** $p < 0.01$, ***$p < 0.001$, **** $p < 0.0001$ repeated measures ANOVA and Holm-Sidak multiple comparison test. Error bars = SEM.

## Tables

**Table 1: Action potential properties of $G_q$-DREADD intra-articularly transduced knee neurons.** RMP = Resting membrane potential, HPD = Half peak duration. * = $p < 0.05$ unpaired t-test.

| | **Ctrl (n = 19)** | | **C21 (n = 18)** | |
|---|---|---|---|---|
| | Mean | SEM | Mean | SEM |
| **RMP (mV)** | -40.8 | 3.0 | -42.7 | 2.8 |
| **Threshold (pA)** | 415.8 | 69.7 | 211.1* | 51.4 |
| **HPD (ms)** | 2.6 | 0.5 | 1.9 | 0.3 |
| **Afterhyperpolarization amplitude (AHP peak, mV)** | 14.7 | 2.1 | 16.8 | 2.8 |

**Table 2: Action potential properties of $G_i$-DREADD intra-articularly transduced knee neurons.** RMP = resting membrane potential, HPD = Half peak duration. * = $p < 0.05$ CFA vs. Ctrl, $$ = $p < 0.01$ CFA vs. CFA+C21, unpaired t-test.

| | **Ctrl (n = 22)** | | **CFA (n = 20)** | | **CFA + C21 (n = 22)** | |
|---|---|---|---|---|---|---|
| | Mean | SEM | Mean | SEM | Mean | SEM |
| **RMP (mV)** | -42.9 | 2.9 | -39.2 | 2.7 | -39.5 | 2.7 |
| **Threshold (pA)** | 418.2* | 65.6 | 242.5 | 45.0 | 536.4$$ | 66.5 |
| **HPD (ms)** | 2.4 | 0.6 | 2.9 | 0.5 | 2.1 | 0.3 |
| **Afterhyperpolarization amplitude (AHP peak, mV)** | 12.9 | 1.3 | 16.5 | 1.3 | 13.8 | 1.6 |

# Figure 1

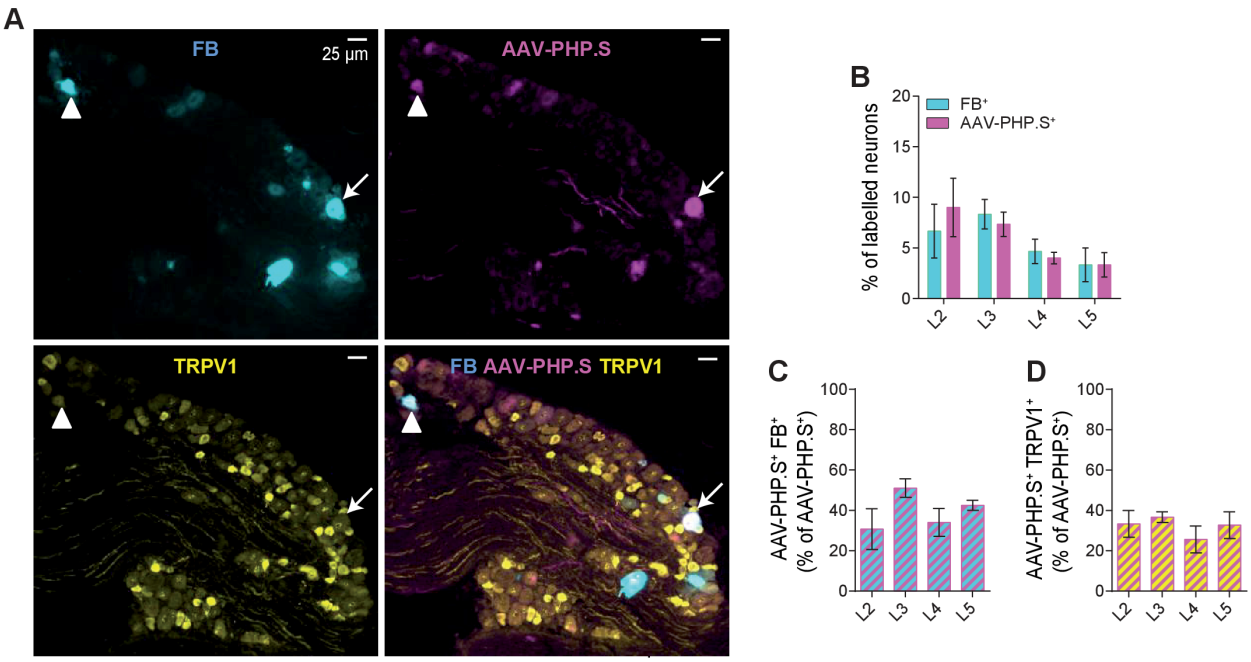
A
FB
25 µm
AAV-PHP.S
TRPV1
FB AAV-PHP.S TRPV1
B
% of labelled neurons
FB+
AAV-PHP.S+
L2
L3
L4
L5
C
AAV-PHP.S+ FB+
(% of AAV-PHP.S+)
D
AAV-PHP.S+ TRPV1+
(% of AAV-PHP.S+)

# Figure 2

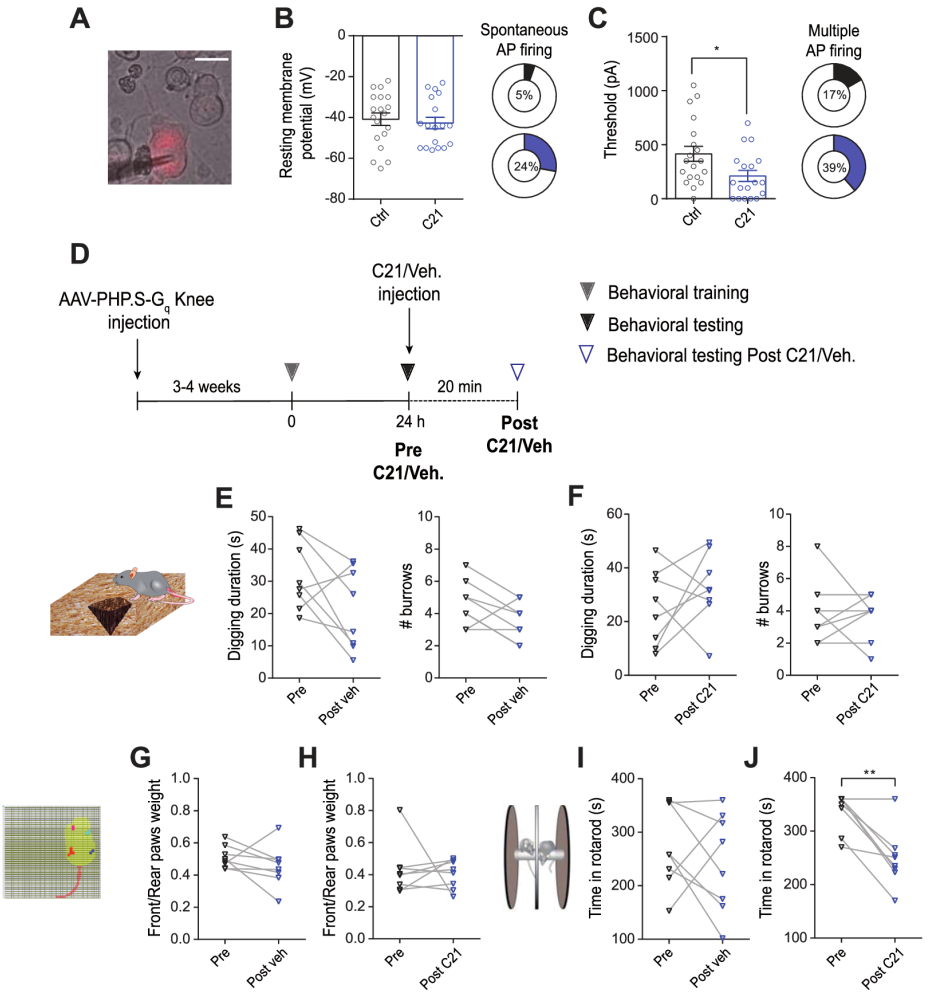
A
B
Resting membrane potential (mV)
0
-20
-40
-60
-80
Ctrl
C21
Spontaneous AP firing
5%
24%
C
Threshold (pA)
1500
1000
500
0
*
Ctrl
C21
Multiple AP firing
17%
39%
D
AAV-PHP.S-Gq Knee injection
3-4 weeks
0
C21/Veh. injection
20 min
24 h
Pre C21/Veh.
Post C21/Veh
Behavioral training
Behavioral testing
Behavioral testing Post C21/Veh.
E
Digging duration (s)
# burrows
Pre
Post veh
F
Digging duration (s)
# burrows
Pre
Post C21
G
Front/Rear paws weight
Pre
Post veh
H
Front/Rear paws weight
Pre
Post C21
I
Time in rotarod (s)
Pre
Post veh
J
**
Time in rotarod (s)
Pre
Post C21

# Figure 3

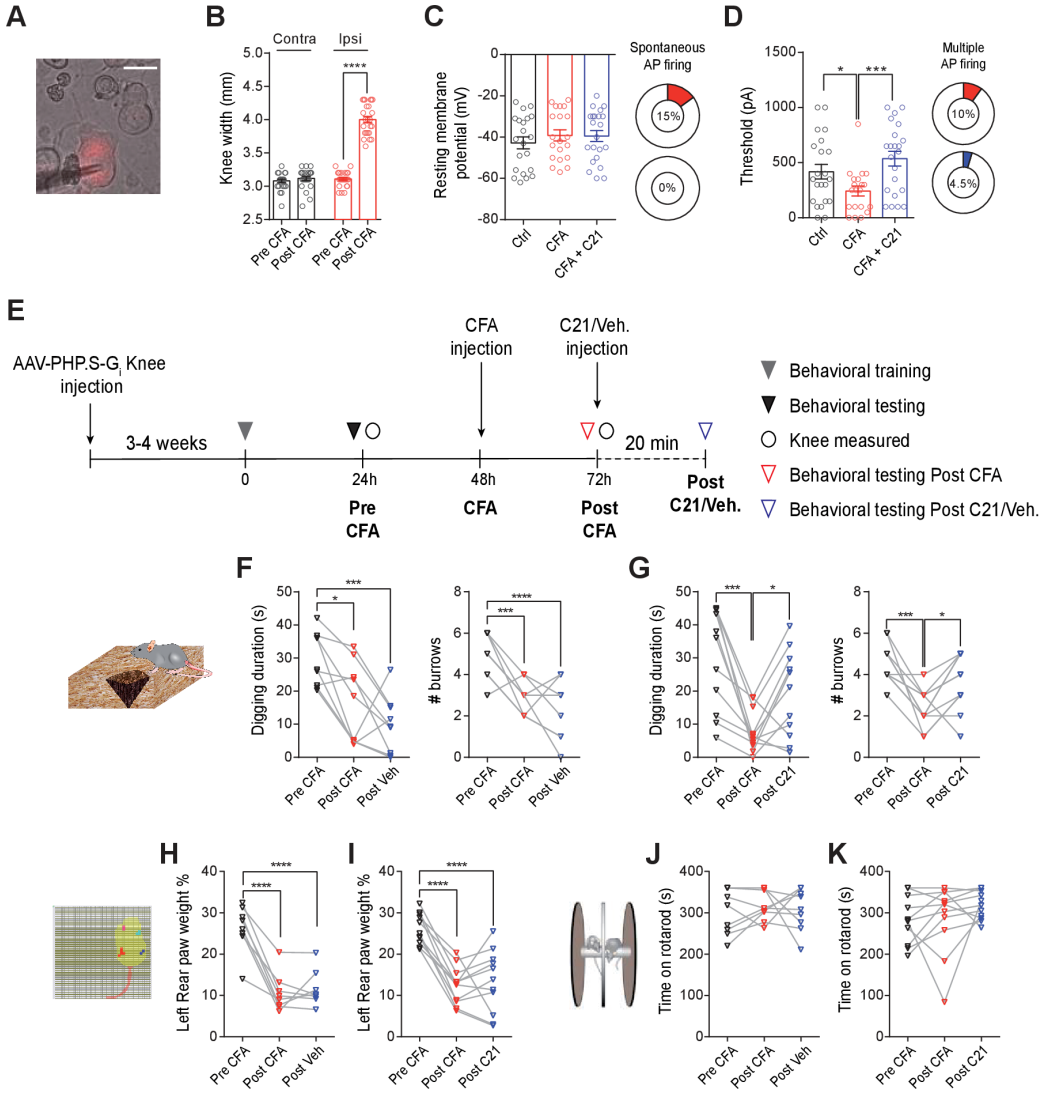
A
B
Contra
Ipsi
Knee width (mm)
Pre CFA
Post CFA
C
Resting membrane potential (mV)
Ctrl
CFA
CFA + C21
Spontaneous AP firing
15%
0%
D
Threshold (pA)
Multiple AP firing
10%
4.5%
E
AAV-PHP.S-G$_i$ Knee injection
3-4 weeks
CFA injection
C21/Veh. injection
20 min
Pre CFA
CFA
Post CFA
Post C21/Veh.
Behavioral training
Behavioral testing
Knee measured
Behavioral testing Post CFA
Behavioral testing Post C21/Veh.
F
Digging duration (s)
# burrows
Post Veh
G
Post C21
H
Left Rear paw weight %
I
J
Time on rotarod (s)
K

**Figure S1**

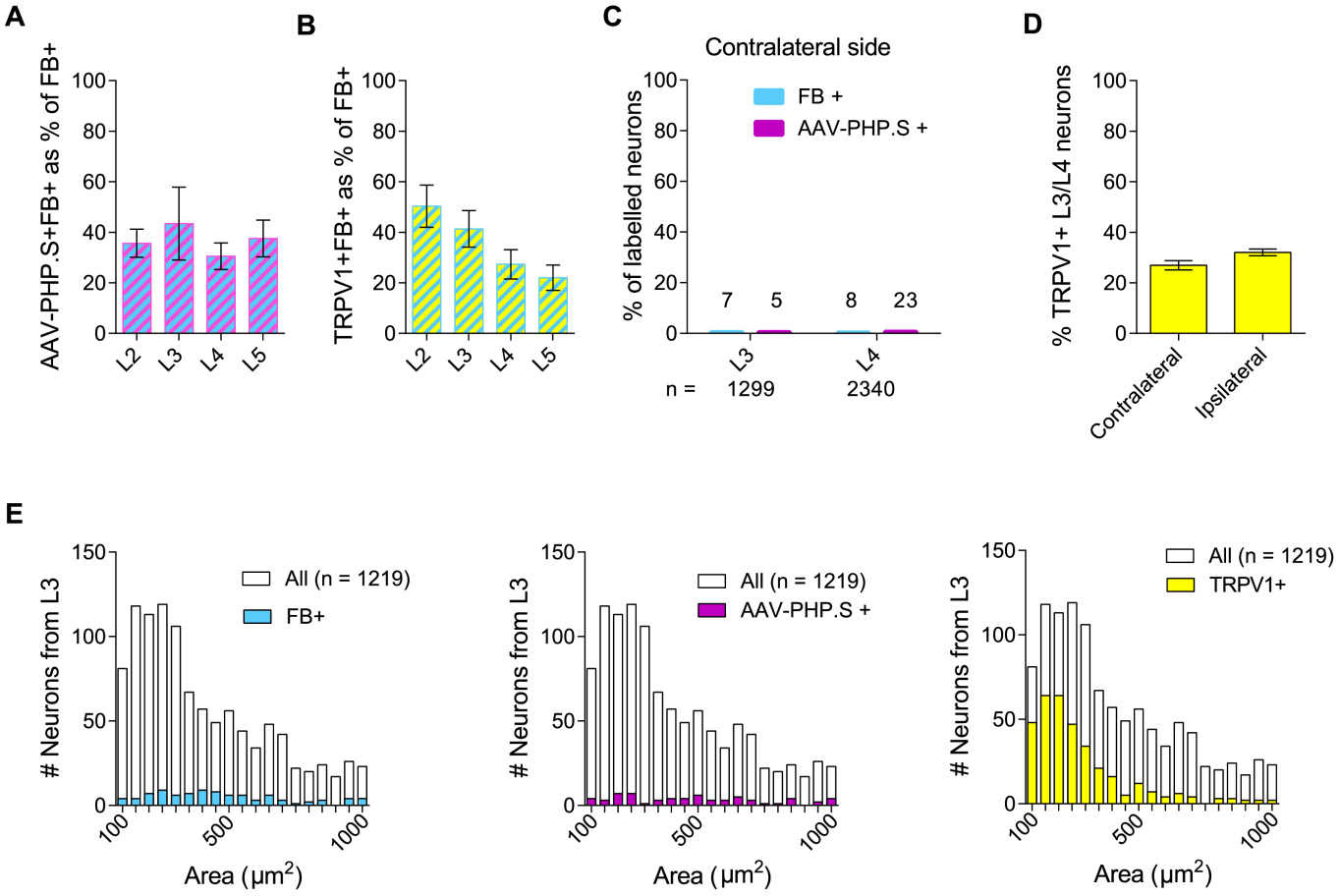
A
AAV-PHP.S+FB+ as % of FB+
100
80
60
40
20
0
L2
L3
L4
L5
B
TRPV1+FB+ as % of FB+
C
Contralateral side
FB +
AAV-PHP.S +
% of labelled neurons
7
5
8
23
L3
L4
n =
1299
2340
D
% TRPV1+ L3/L4 neurons
Contralateral
Ipsilateral
E
# Neurons from L3
All (n = 1219)
FB+
AAV-PHP.S +
TRPV1+
150
100
50
0
100
500
1000
Area (µm²)

# Figure S2

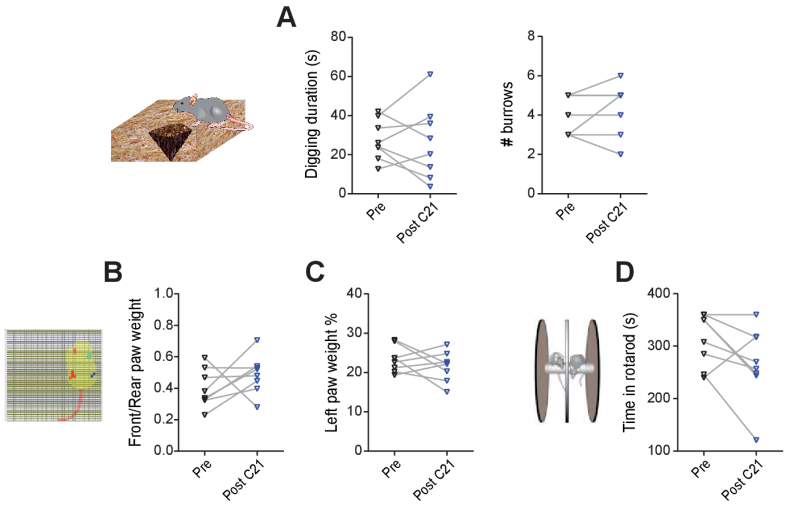
A
Digging duration (s)
80
60
40
20
0
Pre
Post C21
# burrows
8
6
4
2
0
Pre
Post C21
B
Front/Rear paw weight
1.0
0.8
0.6
0.4
0.2
0.0
Pre
Post C21
C
Left paw weight %
40
30
20
10
0
Pre
Post C21
D
Time in rotarod (s)
400
300
200
100
Pre
Post C21

# Figure S3

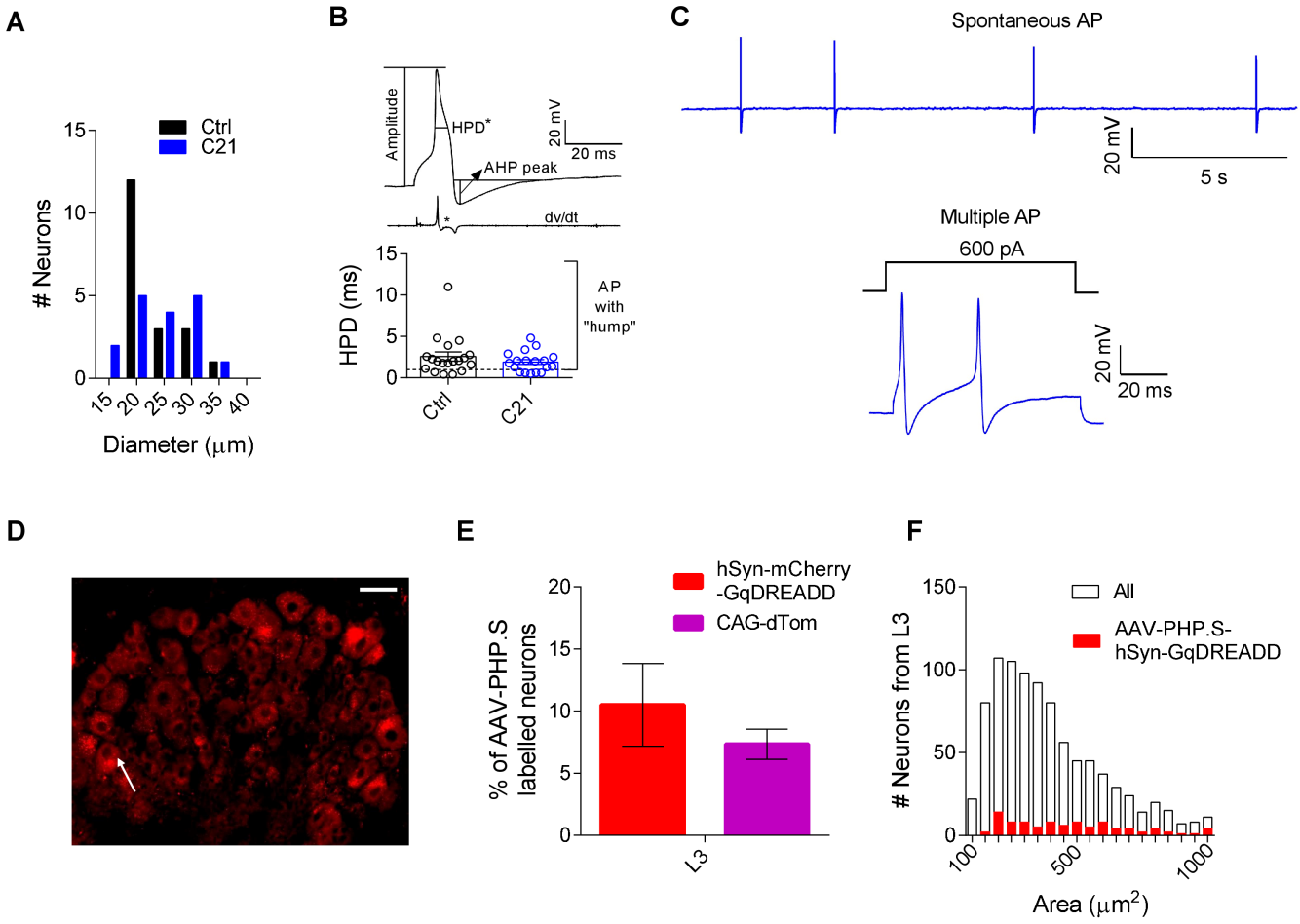
A
Ctrl
C21
# Neurons
Diameter (μm)
B
Amplitude
HPD*
AHP peak
dv/dt
20 mV
20 ms
HPD (ms)
AP with "hump"
Ctrl
C21
C
Spontaneous AP
20 mV
5 s
Multiple AP
600 pA
20 mV
20 ms
D
E
hSyn-mCherry -GqDREADD
CAG-dTom
% of AAV-PHP.S labelled neurons
L3
F
All
AAV-PHP.S-hSyn-GqDREADD
# Neurons from L3
Area (μm²)

# Figure S4

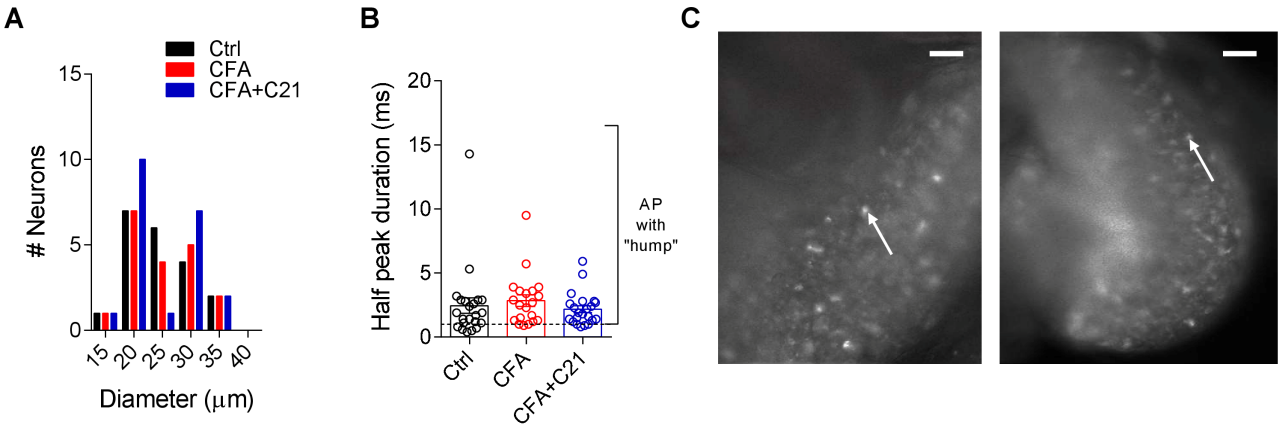
A
Ctrl
CFA
CFA+C21
# Neurons
15
10
5
0
15
20
25
30
35
40
Diameter (μm)
B
Half peak duration (ms)
20
15
10
5
0
AP
with
"hump"
Ctrl
CFA
CFA+C21
C